R. Pittau

Granada, January 2007

1

High Energy hadronic collisions at the LHC

http://hands-on-cern.physto.se/ani/acc_lhc_atlas/lhc_atlas.swf

The Factorization Theorem

$$\frac{d\sigma}{dX} = \sum_{j,k} \int_{\hat{X}} f_j(x_1, Q_i) f_k(x_2, Q_i) \frac{d\hat{\sigma}_{j,k}(Q_i, Q_f)}{d\hat{X}} F(\hat{X} \to X; Q_i, Q_f)$$

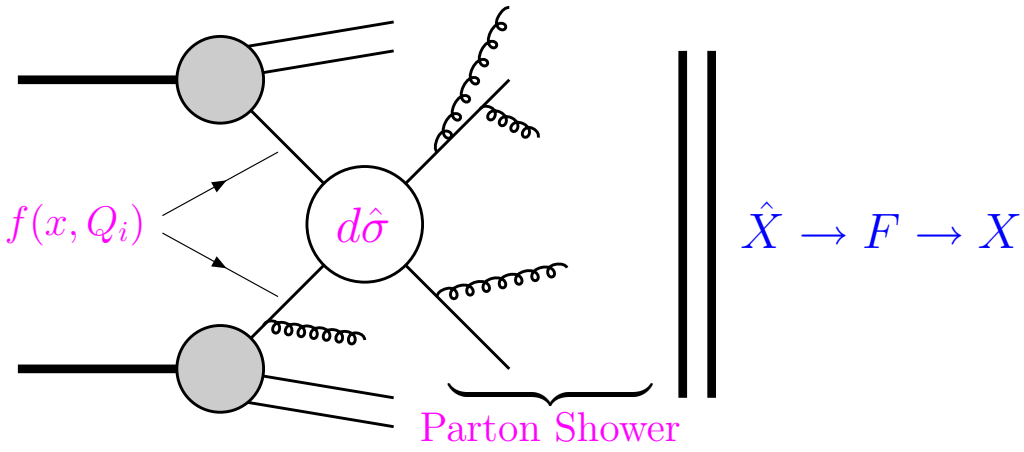

$f \Rightarrow$ Sum over all initial state histories leading to $p_j = xP_{proton}$.

$F \Rightarrow$ Transition from partonic final state to the hadronic observable.

$$\frac{d\sigma}{dX} = \sum_{j,k} \int_{\hat{X}} f_j(x_1, Q_i) f_k(x_2, Q_i) \frac{d\hat{\sigma}_{j,k}(Q_i, Q_f)}{d\hat{X}} F(\hat{X} \to X; Q_i, Q_f)$$

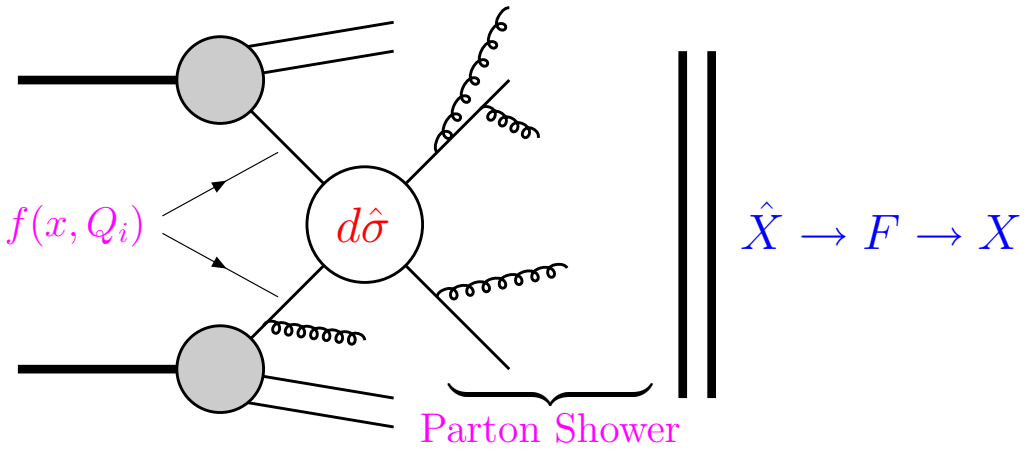

The Matrix Element computation (at the tree level)

1) Elicity Methods

2) The Dyson Schwigner approach

Helicity Methods

• One evaluates directly the amplitudes as complex numbers (instead of squaring them) ⇒

explicit representations of the wave functions of the external particles (ϵ_μ, u, v) *are needed* :

• Massless vector:

$$\epsilon_\mu^{(\lambda)}(k) = \frac{1}{\sqrt{2}} \frac{\bar{u}_\lambda(k)\gamma_\mu u_\lambda(n)}{\bar{u}_{-\lambda}(n)u_\lambda(k)}\,, \qquad n^2 = 0\,, \quad \lambda = \pm\,.$$

- Massless (Weyl) spinors:

$$v_-(1) = u_+(1) = 1_{\rm A} \qquad \bar{v}_-(1) = \bar{u}_+(1) = 1_{\dot{\rm A}}$$
$$v_+(1) = u_-(1) = 1^{\dot{\rm A}} \qquad \bar{v}_+(1) = \bar{u}_-(1) = 1^{\rm A}$$

$(\frac{1}{2}, 0) + (0, \frac{1}{2})$ *$SL(2, C)$ representation of the Lorentz group.*

- γ matrices (Weyl representation):

$$\gamma_\mu = \begin{pmatrix} 0 & \sigma_{\mu \dot{\rm B} {\rm A}} \\ \sigma_\mu^{\dot{\rm A} {\rm B}} & 0 \end{pmatrix} , \qquad \gamma_5 = \begin{pmatrix} \sigma_0 & 0 \\ 0 & -\sigma_0 \end{pmatrix} .$$

see e.g. J.G.M. Kuijf, Ph.D. Thesis, RX-1335, LEIDEN, (1991)

- Basic rules and spinorial inner products:

$$\sigma_\mu^{\dot{\rm A}\rm B}\sigma^{\mu\dot{\rm C}\rm D} = 2\,\epsilon^{\dot{\rm A}\dot{\rm C}}\epsilon^{\rm BD}\,, \quad \epsilon^{\rm AB} = \begin{pmatrix} 0 & 1 \\ -1 & 0 \end{pmatrix} = \epsilon_{\rm AB} = \epsilon^{\dot{\rm A}\dot{\rm B}} = \epsilon_{\dot{\rm A}\dot{\rm B}}\,,$$

$$\epsilon_{\rm AB} \equiv -\epsilon_{\rm BA}\,, \quad 1^{\rm B} = 1_{\rm A}\epsilon^{\rm AB}\,, \quad < 12 > \equiv 1_{\rm A}2^{\rm A}\,, \quad [12] \equiv 1_{\dot{\rm A}}2^{\dot{\rm A}}\,,$$

$$< 12 > [12] = 2\,p_1 \cdot p_2\,.$$

• Example $e^+e^- \to \mu^+\mu^-$ in QED (all incoming momenta and massless particles):

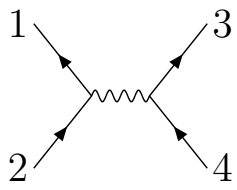

$$A(++) \;\propto\; \bar{v}_+(1)\gamma_\mu u_-(2)\,\bar{v}_+(3)\gamma^\mu u_-(4) = 1^{\rm A}\,2^{\dot{\rm B}}\,3^{\rm C}\,4^{\dot{\rm D}}\;\sigma_{\mu\dot{\rm B}\rm A}\sigma^{\mu}_{\dot{\rm D}\rm C}$$

$$= \;2\;1^{\rm A}\,2^{\dot{\rm B}}\,3^{\rm C}\,4^{\dot{\rm D}}\epsilon_{\dot{\rm B}\dot{\rm D}}\epsilon_{\rm AC} = 2\;[42] < 31 > \;.$$

• Helicity techniques based on spinorial inner products are successfully used also in one-loop calculations (but care is necessary when using dimensional regularization).

• Although each diagram can be computed efficiently multi-particle amplitudes involve the evaluation of an exceedingly large numbers of Feynamn diagrams. *e.g.*

Process	$n = 7$	$n = 8$	$n = 9$	$n = 10$
$g\ g \to n\ g$	559,405	10,525,900	224,449,225	5,348,843,500
$q\bar{q} \to n\ g$	231,280	4,016,775	79,603,720	1,773,172,275

Table 1: Number of Feynman diagrams corresponding to amplitudes with different numbers of quarks and gluons.

F. Caravaglios, M. L. Mangano, M. Moretti and R. P., NPB 539 (1999) 215

A pure numerical approach to the calculations of transition amplitudes is welcome. This can be done with the ALPHA algorithm

F. Caravaglios and M. Moretti, PLB 358 (1995) 332

The Idea: The Matrix Element 'is' the Legendre Transform Z of the (effective) Lagrangian Γ (1PI Green Functions generator) $\rightarrow$ the problem can be re-casted as a *minimum problem*, more suitable for a *numerical approach* (DS equation).

The Dyson-Schwinger equations

F. A. Berends and W. Giele, NPB 306 (1988) 759
A. Kanaki and C. G. Papadopoulos, hep-ph/0012004

An alternative to the Feynman graph representation is provided by the Dyson-Schwinger approach.

Dyson-Schwinger equations express recursively the n-point Green's functions in terms of the $1-, 2-, \ldots, (n-1)$-point functions.

• Imagine a 0-dimensional universe with only one point ϕ. The Quantum Field Theory describing such a system is comlpetely specified by all possible p-point (Euclidean) Green Functions:

$$G_p \equiv < \phi^p > = N \int d\phi \, \phi^p \, e^{-S(\phi)} \, .$$

• They can be obtained from a *Generating Functional* as follows:

$$Z(J) = N \int d\phi \, e^{-S(\phi)+J\phi} = \sum_{p \geq 0} G_p \frac{J^p}{p!} \, .$$

• The DS Equations follow from the standard identity that the integral of a derivative is zero:

$$\begin{aligned} 0 &= N \int d\phi \frac{d}{d\phi} \left\{ e^{-S(\phi)+J\phi} \right\} \\ &= N \int d\phi \left\{ -S'(\phi) + J \right\} e^{-S(\phi)+J\phi} \\ &= \left\{ -S'(\partial_J) + J \right\} Z(J) \, . \end{aligned}$$

• Therefore one obtains the following *Dyson-Schwinger* equations:

$$S'(\partial_J)Z = JZ(J)\,.$$

• For instance in QED these equations can be graphically represented as follows:

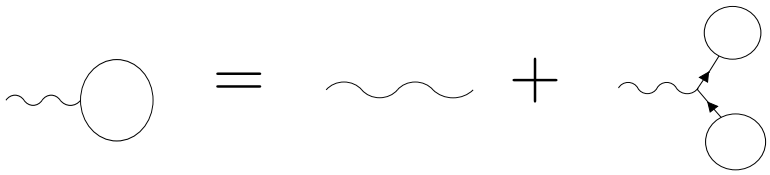

• This gives rise to a recursive algorithm easily implementable in a Computer Code (`ALPGEN`).

$$\frac{d\sigma}{dX} = \sum_{j,k} \int_{\hat{X}} f_j(x_1, Q_i) f_k(x_2, Q_i) \frac{d\hat{\sigma}_{j,k}(Q_i, Q_f)}{d\hat{X}} F(\hat{X} \to X; Q_i, Q_f)$$

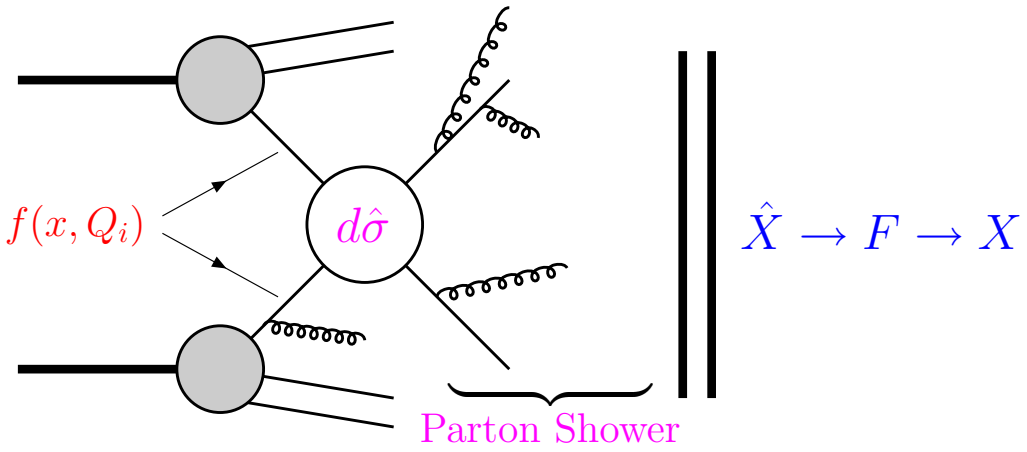

The convolution with the pdf's

• To complete the calculation, one needs to perform the integration over the *parton distribution functions*

• Those distribution functions are extracted from deep inelastic scattering data

see e.g. S. Willenbrock, BNL-43793 (1990)

• They are available as prepackaged computer programs, that can be used to perform the integral numerically. The most popular sets are:

- CTEQ

J. Pumplin *et al.*, JHEP **0207**, 012 (2002)

- MRST

A. D. Martin, R. G. Roberts, W. J. Stirling and R. S. Thorne, Eur. Phys. J. C **14**, 133 (2000)

$$\frac{d\sigma}{dX} = \sum_{j,k} \int_{\hat{X}} f_j(x_1, Q_i) f_k(x_2, Q_i) \frac{d\hat{\sigma}_{j,k}(Q_i, Q_f)}{d\hat{X}} F(\hat{X} \to X; Q_i, Q_f)$$

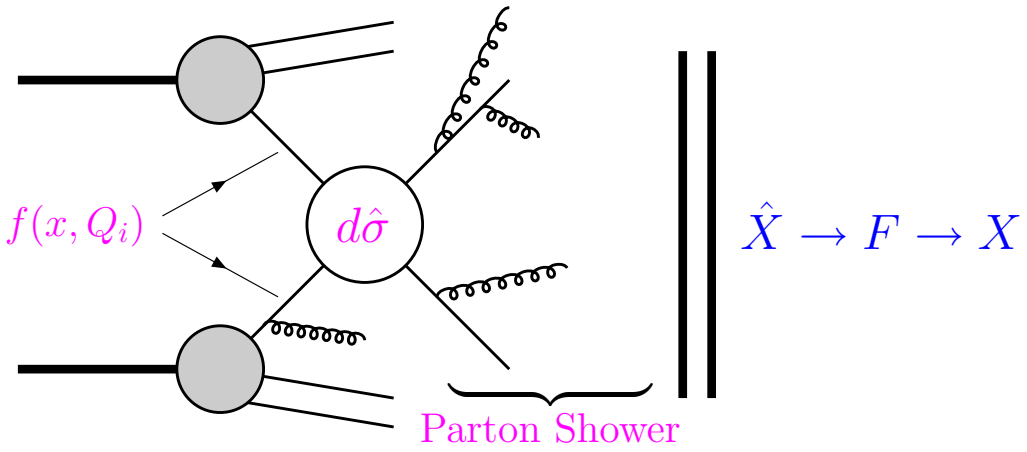

Subprocess selection

•The calculation of the cross section for multi-parton final states involves typically the sum over a large set of subprocesses and flavour configurations *e.g.* for the $Wb\bar{b}$ final state:

jp	subprocess	jp	subprocess	jp	subprocess
1	$q\bar{q}' \to WQ\overline{Q}$	2	$qg \to q'WQ\overline{Q}$	3	$gq \to q'WQ\overline{Q}$
4	$gg \to q\bar{q}'WQ\overline{Q}$	5	$q\bar{q}' \to WQ\overline{Q}q''\bar{q}''$	6	$qq'' \to WQ\overline{Q}q'q''$
7	$q''q \to WQ\overline{Q}q'q''$	8	$q\bar{q} \to WQ\overline{Q}q'\bar{q}''$	9	$q\bar{q}' \to WQ\overline{Q}q\bar{q}$
10	$\bar{q}'q \to WQ\overline{Q}q\bar{q}$	11	$q\bar{q} \to WQ\overline{Q}q\bar{q}'$	12	$q\bar{q} \to WQ\overline{Q}q'\bar{q}$
13	$qq \to WQ\overline{Q}qq'$	14	$qq' \to WQ\overline{Q}qq$	15	$qq' \to WQ\overline{Q}q'q'$
16	$qg \to WQ\overline{Q}q'q''\bar{q}''$	17	$gq \to WQ\overline{Q}q'q''\bar{q}''$	18	$qg \to WQ\overline{Q}qq\bar{q}'$
19	$qg \to WQ\overline{Q}q'q\bar{q}$	20	$gq \to WQ\overline{Q}qq\bar{q}'$	21	$gq \to WQ\overline{Q}q'q\bar{q}$
22	$gg \to WQ\overline{Q}q\bar{q}'q''\bar{q}''$	23	$gg \to WQ\overline{Q}q\bar{q}q\bar{q}'$		

Each of these subprocesses receives contributions from several possible flavour configurations (e.g. $u\bar{d} \to WQ\overline{Q}gg$ *,* $u\bar{s} \to WQ\overline{Q}gg$*, etc.)*

• The subdivision in subprocesses can be designed to allow to sum the contribution of different flavour configurations by simply adding trivial factors such as parton densities or CKM factors, which factorize out of a single, flavour independent, matrix element.

• For example the overall contribution from the 1^{st} process in the list is given by

$$\left[u_1\bar{d}_2\cos^2\theta_c + u_1\bar{s}_2\sin^2\theta_c + c_1\bar{s}_2\cos^2\theta_c + c_1\bar{d}_2\sin^2\theta_c\right] \times |M(q\bar{q}' \to WQ\overline{Q}gg)|^2$$

where $q_i = f(x_i),\ i = 1, 2$, are the parton densities for the quark flavour q. Contributions from charge-conjugate or isospin-rotated states can also be summed up, after trivial momentum exchanges.

• For example, the same matrix element calculation is used to describe the four events:

$$
\begin{aligned}
u(p_1)\bar{d}(p_2) &\rightarrow b(p_3)\bar{b}(p_4)g(p_5)g(p_6)e^+(p_5)\nu(p_6) \\
\bar{u}(p_1)d(p_2) &\rightarrow \bar{b}(p_3)b(p_4)g(p_5)g(p_6)e^-(p_5)\bar{\nu}(p_6) \\
\bar{d}(p_1)u(p_2) &\rightarrow \bar{b}(p_3)b(p_4)g(p_5)g(p_6)\nu(p_5)e^+(p_6) \\
d(p_1)\bar{u}(p_2) &\rightarrow b(p_3)\bar{b}(p_4)g(p_5)g(p_6)\bar{\nu}(p_5)e^-(p_6)
\end{aligned}
$$

• Event by event, the flavour configuration for the assigned subprocess is then selected with a probability proportional to the relative size of the individual contributions to the luminosity, weighted by the Cabibbo angles.

$$\frac{d\sigma}{dX} = \sum_{j,k} \int_{\hat{X}} f_j(x_1, Q_i) f_k(x_2, Q_i) \frac{d\hat{\sigma}_{j,k}(Q_i, Q_f)}{d\hat{X}} F(\hat{X} \to X; Q_i, Q_f)$$

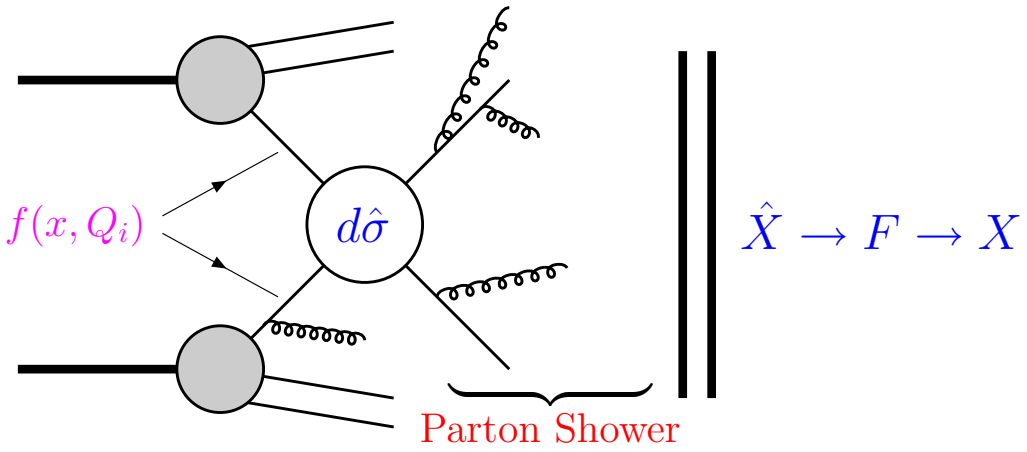

The perturbative Parton Shower

• It is important because a lot of final state jets are typically observed, in hadronic collisions, coming from QCD radiation that, subsequently, hadronizes. It is still pertubatively calculable by introducing the so called *Sudakov Form Factors*.

• In QED (at the LL):

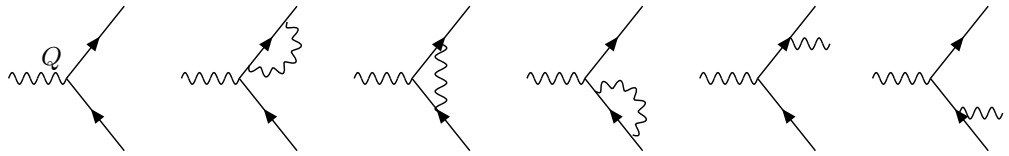

$$= d\sigma_0 \left(1 - \frac{\alpha}{\pi} \log^2 \frac{Q}{Q_0}\right) , \qquad Q > Q_0 > 0 ,$$

where the $\log^2$ comes from the overlap of soft and collinear emissions.

• Thanks to factorization theorems one can exponentiate this result to get

$$d\sigma_{rad} = d\sigma_0 \; exp\left\{-\frac{\alpha}{\pi}\log^2\frac{Q}{Q_0}\right\} .$$

• In QCD (at the LL): $\alpha \to C_F\alpha_s, \quad C_F = \frac{N_c^2-1}{2N_c} = \frac{4}{3}$ and

$$d\sigma_{rad} = d\sigma_0 \; exp\left\{-\frac{\alpha_s C_F}{\pi}\log^2\frac{Q}{Q_0}\right\} .$$

• The term

$$exp\left\{-\frac{\alpha_s C_F}{\pi}\log^2\frac{Q}{Q_0}\right\}$$

represents the probability for a quark of $\underline{NOT}$ radiating any gluon when passing from a scale Q to a scale $Q_0 < Q$.

• In reality $\alpha_s = \alpha_s(Q)$ and one defines

$$\Delta_q(Q_0, Q) \equiv exp\left\{ - \int_{Q_0}^{Q} dq\, \Gamma_q(q, Q) \right\} ,$$

where

$$\Gamma_q(q, Q) = \frac{2C_F}{\pi} \frac{\alpha_s}{q} \left(\log \frac{Q}{q} - \frac{3}{4} \right) = P(q \to qg)$$

is the $q \to qg$ Altarelli-Parisi splitting function.

• *When α_s is a constant, taking the integral reproduces the previous expression (at the LL).*

• Analogously, with

$$\Gamma_g(q,Q) = P(g \to gg) \quad \text{and} \quad \Gamma_f(q) = P(g \to q\bar{q})\,,$$

one defines a Sudakov Form factor for the gluon

$$\Delta_q(Q_0,Q) \equiv expx\left\{-\int_{Q_0}^{Q} dq\,[\Gamma_g(q,Q)+\Gamma_f(q)]\right\}\,.$$

• Knowing the $\Delta_{q,g}(Q_0,Q)$ one can easily construct Monte-Carlo programs to explicitly generate the perturbative Parton Shower cascade (in principle including an infinite number of emissions).

• However the results will be only reliable in the soft/collinear regime. Outside one should calculate the exact Matrix elements

$$\Rightarrow \text{possible double counting problem}$$

$$\Rightarrow \text{CKKW and Matching à la MLM (see later)}$$

• In QCD, at each colour flow corresponds a different structure of Sudakov Form Factors $\Rightarrow$

Reconstruction of colour flows

• The emission of soft gluon radiation in shower MC programs accounts for quantum coherence, which is implemented via the prescription of angular ordering in the parton cascade.

• The colour flow is the set of colour connections among the partons which defines the set of dipoles for a given event.

• In order to reliably evolve a multi-parton state into a multi-jet configuration, it is necessary to associate a specific colour-flow pattern to each generated parton-level event.

• Consider for example the case of multigluon processes. The scattering amplitude for n gluons with momenta p_i^μ, helicities ϵ_i^μ and colours a_i (with $i = 1, \ldots, n$), can be written as

F.A. Berends and W. Giele, NPB 294 (1987) 700

M. Mangano, S. Parke and Z. Xu, NPB 298 (1988) 653

$$M(\{p_i\}, \{\epsilon_i\}, \{a_i\}) = \sum_{P(2,3,\ldots,n)} \mathrm{tr}(\lambda^{a_{i_1}} \lambda^{a_{i_2}} \ldots \lambda^{a_{i_n}}) A(\{p_{i_1}\}, \{\epsilon_{i_1}\}; \ldots \{p_{i_n}\}, \{\epsilon_{i_n}\}) \,.$$

• The functions $A(\{P_i\})$ (known as *dual* or *colour-ordered* amplitudes) are gauge-invariant, cyclically-symmetric functions of the gluons' momenta and helicities.

• Each dual amplitude $A(\{P_i\})$ corresponds to a set of diagrams where colour flows from one gluon to the next, according to the ordering specified by the permutation of indices.

• When summing over colours the amplitude squared, different orderings of dual amplitudes are orthogonal at the leading order in $1/N^2$

$$\sum_{\mathrm{col's}} |M(\{p_i\},\{\epsilon_i\},\{a_i\})|^2 \;=\; N^{n-2}(N^2-1)\sum_{P_i}\left[|A(\{P_i\})|^2+\frac{1}{N^2}(\mathrm{interf.})\right] .$$

• At the leading order in $1/N^2$, therefore, the square of each dual amplitude is proportional to the relative probability of the corresponding colour flow

• Each flow defines, in a gauge invariant way, the set of colour currents which are necessary and sufficient to implement the colour ordering prescription necessary for the coherent evolution of the gluon shower.

• Because of the incoherence of different colour flows, each event can be assigned a specific colour configuration by comparing the relative size of $|A(\{P_i\})|^2$ for all possible flows.

• When working at the physical value of $N_c = 3$, the interferences among different flows cannot be neglected in the evaluation of the square of the matrix element. As a result, the basis of colour flows does not provide an orthogonal set of colour states:

Our solution for and efficient color flow generation including $1/N$ corrections in the Matrix Element evaluation

$\Rightarrow$

- Choose a standard $SU(3)$ orthonormal basis (Gell-Mann matrices for example).

- Randomly select a non-vanishing colour assignment for the external gluons.

- *If the event is accepted* choose randomly among the *contributing* dual amplitudes a color flow on the basis of their relative weight.

• Two advantages:

1) Dual amplitudes required only for a small number of phase space points.

2) Contributing dual amplitudes to a given external coulor assignment $\ll$ than total number.

The CKKW algorithm

• As an example take $e^+e^- \to n$-jets.

• First recall that, in QCD, two objects i and j are resolved (using the k_T algorithm) if

$$y_{ij} \equiv 2 \min\{E_i^2, E_j^2\}(1 - \cos\theta_{ij})/Q^2 > y_{cut}. \qquad (1)$$

• One can reproduce (at the LL accuracy) the e^+e^-n-jet fractions at the k_T resolution

$$y_{ini} = \frac{Q_0^2}{Q^2}$$

using a probabilistic diagrammatic (NOT Feynman diagrams) approach as follows:

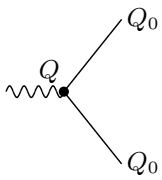

$$\Rightarrow \qquad R_2 = \Delta_q(Q_0, Q)^2$$

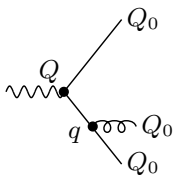

$$\Rightarrow \qquad R_3 = 2\,\Delta_q(Q_0, Q)^2 \int_{Q_0}^{Q} dq\,\Gamma_q(q, Q)\Delta_g(Q_0, q)\,.$$

• If $y_{cut} > y_{ini}$ one can improve the above description by replacing Γ with the appropriate tree-level matrix element squared.

For example, for the 3-jet distribution

$$\Gamma_q(q, Q) \to |M_{q\bar{q}g}|^2\,.$$

In general

• At $y_{cut} > y_{ini}$

1) choose the n-parton configuration with probability proportional to the tree level matrix elements squared $|M_n|^2$;

2) distribute all momenta according to $|M_n|^2$;

3) reconstruct a probabilistic diagram by using the k_T algorithm;

4) reweight $|M_n|^2$ by a product of Sudakov form factors;

5) the argument of the form factors and the running coupling are computed at the typical scales on the nodal values of the reconstructed probabilistic diagram.

• At $y_{cut} < y_{ini}$ one uses instead a parton shower subjected to a 'veto' procedure, which cancels the y_{ini} dependence

$\Rightarrow$ double counting is avoided

The Matching *á la MLM*

- Simpler procedure

1) parton level events are defined by a minimum E_T threshold E_T^{min} for the partons and a minimum separation $\Delta R_{ij} > R_{min}$;

2) a tree structure is reconstructed by using the k_T algorithm, *but using information of the colour flow of the event* ;

3) $\alpha_s(Q_i)$ is computed at the typical scales Q_i on the nodal values of the reconstructed probabilistic diagram;

4) the event is showered (using PYTHIA or HERWIG) *without applying any 'veto' procedure*;

5) *no Sudakow reweighing is applied*, rather, after the showering, a jet cone algorithm (R_{min}, E_T^{min}) is applied and only events where jet and partons match are kept ;

Few examples of matching ($n_{jets} = 3$): hard parton; parton emitted by the shower

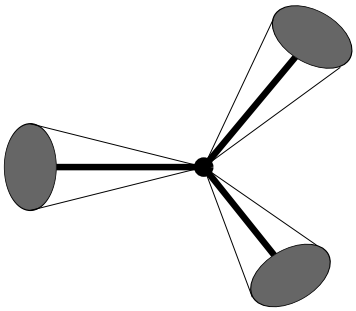

Matched

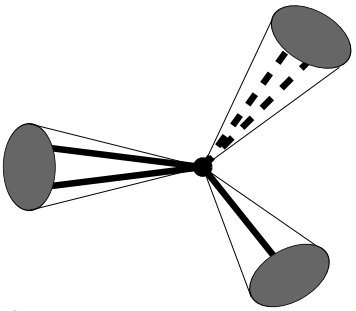

NOT matched: double log double counting

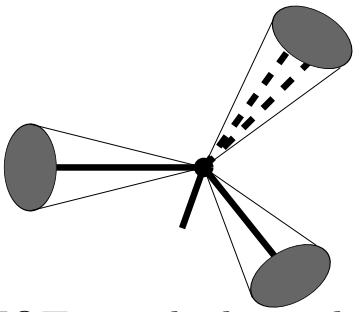

NOT matched: single log double counting

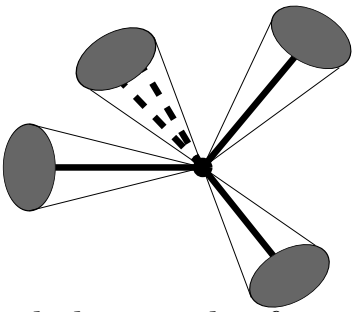

Matched: keep only if $n_{jets} = N_{max}$

6) Events obtained by applying this procedure to the parton level with increasing multiplicity can then be combined to obtain fully inclusive samples spanning a large multiplicity range.

This algorithm is implemented in `ALPGEN` (see later).

R. Pittau

Granada, January 2007

Computing physical observables in hard hadronic collisions at LHC

-Example 1: $Hb\bar{b}$ Yukawa coupling at the LHC

-Example 2: Determination of λ_{HHH} at the (S)LHC

$Hb\bar{b}$ Yukawa coupling at the LHC

M. L. Mangano, M. Moretti, F. Piccinini, R. P. and A. Polosa, Phys. Lett. B556(2003)50

• Study of the $H \to b\bar{b}$ decay in the electroweak boson fusion (WBF) production channel.

• Optimizing the signal significance ($S/\sqrt{B}$) leads to the following set of cuts, on the b jets:

$$p_{\mathrm{T}}^{b} > 30 \text{ GeV}, \quad |\eta_b| < 2.5,$$
$$\Delta R_{bb} > 0.7, \qquad |m_{bb} - m_H| < 0.12 \cdot m_H,$$

and on the forward jets:

$$p_{\mathrm{T}}^{j} > 60\mathrm{GeV}, \qquad |\eta_{j_1} - \eta_{j_2}| > 4.2,$$
$$\Delta R_{jj}\,, \Delta R_{jb} > 0.7, \quad m_{jj} > 1000 \text{ GeV}.$$

• In addition, *two alternative selection criteria for the light-jet rapidities are considered:*

Case $(a) \Rightarrow 2.5 < |\eta_j| < 5$ and $\eta_{j_1}\eta_{j_2} < 0$

Case $(b) \Rightarrow |\eta_j| < 5$

• The background sources considered are:

1. QCD production of $b\bar{b}jj$ final states, where j indicates a jet originating from a light quark (u, d, s, c) or a gluon;
2. QCD production of $jjjj$ final states;
3. Associated production of $Z^*/\gamma^* \to b\bar{b}$ and light jets, where the invariant mass of the $b\bar{b}$ pair is in the Higgs signal region either because of imperfect mass resolution, or because of the high-mass tail of the intermediate vector boson;
4. $t\bar{t}$ and $t\bar{t}j$ production;
5. $b\bar{b}jj$ and $jjjj$ production via *overlapping events.*

Results

• Assuming that the coupling HWW is the one predicted by the SM or determined in other reactions:

	m_H	115 GeV	120 GeV	140 GeV
(a)	$\delta\Gamma_b/\Gamma$	0.33	0.35	0.71
	$\delta y_{Hbb}/y_{Hbb}$	0.58	0.51	0.56
(b)	$\delta\Gamma_b/\Gamma$	0.20	0.19	0.37
	$\delta y_{Hbb}/y_{Hbb}$	0.36	0.30	0.29

• A luminosity of 600 fb^{-1} is assumed with a b mistagging efficiency $\epsilon_{fake} = 0.01$.

• $\epsilon_{fake} = 0.05$ would worsen these estimates by approximately 20%.

Determination of λ_{HHH} at LHC

M. Moretti, S. Moretti, F. Piccinini, R. P. and A. Polosa, hep-ph/0410334 and hep-ph/0411039

• The complete reconstruction of the SM Higgs potential necessarily requires the measurement of the Higgs self-couplings:

$$\lambda^{(0)}_{HHH} = -3\,\frac{M_H^2}{v}\,, \quad \lambda^{(0)}_{HHHH} = -3\,\frac{M_H^2}{v^2}\,, \quad (v = 246 \text{ GeV})$$

• The leading production channels of Higgs boson pairs at hadron colliders are

$$\begin{aligned} gg &\to HH \ (gg \text{ fusion}) \\ gg, q\bar{q} &\to Q\bar{Q}HH \ \ (\text{heavy} - \text{quark associated production}) \\ qq^{(\prime)} &\to qq^{(\prime)}HH \ (\text{vector} - \text{vector fusion}) \\ q\bar{q}^{(\prime)} &\to VHH \ (\text{Higgs} - \text{strahlung}) \end{aligned}$$

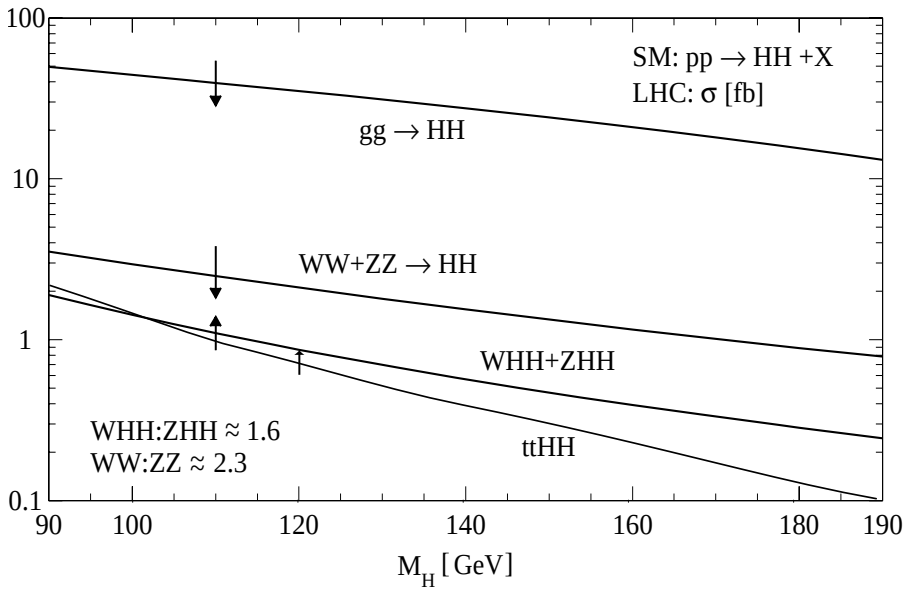

Figure 1: *Cross sections for Higgs pair production in the SM via gg fusion, vector-vector fusion and Higgs-strahlung, plus heavy-quark associated production. The vertical arrows correspond to a variation of λ_{HHH} from 1/2 to 3/2 of the SM value.*

• Different decay channels dominate the final state, depending on the value of M_H:

- 120 GeV $\lesssim M_H \lesssim$ 140 GeV (IMH) $\Rightarrow H \to b\bar{b}$

- $M_H \gtrsim$ 140 GeV $\Rightarrow H \to W^{\pm(*)}W^{\mp}$ and $H \to Z^{(*)}Z$

IMH

• IMH boson pairs via $gg \to HH \to b\bar{b}b\bar{b}$ within the SM is most probably not feasible at the LHC and very difficult at the so-called SLHC* the tenfold luminosity increase option of the LHC (for a heavier Higgs boson the situation is much brighter)

U. Baur, T. Plehn and D. Rainwater, Phys. Rev. **D68** (2003) 033001

* F. Gianotti, M.L. Mangano, T. Virdee (conveners), `hep-ph/0204087`

• We present here the first results of studies performed specifically in the case of IMH boson pairs produced via the other three production modes.

- IMH is still quite possible:

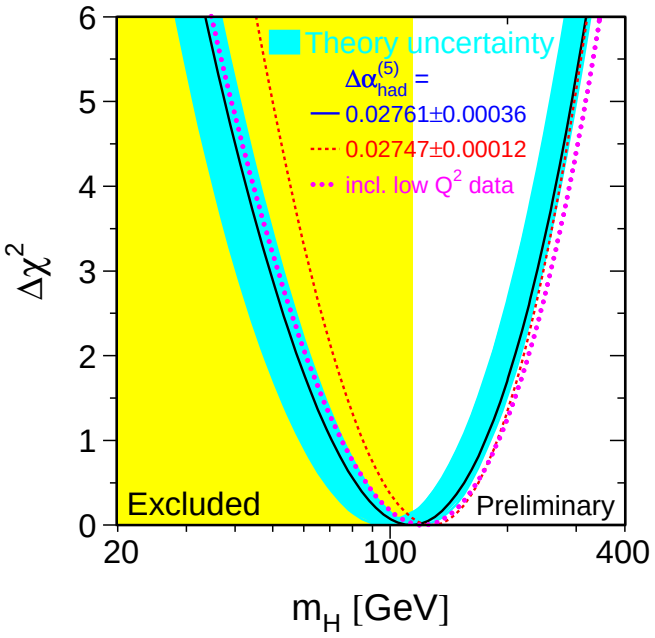

Figure 2: *Precision data vs. direct Higgs searches at LEP (Winter 2004).*

• A detailed signal-to-background analysis performed with ALPGEN shows that the available statistics is in general too low for quantitative SM estimates of $\lambda^{(0)}_{HHH}$ at the LHC with 300 fb^{-1} of accumulated luminosity.

• However, there are models beyond SM, that can "look alike" the SM in their decoupling limit:

general type II CP-conserving THDM

J. F. Gunion and H. E. Haber, Phys. Rev. **D67** (2003) 075019.

• The lightest Higgs (among the 5 Higgses) "look alike" the SM Higgs, while the heavy modes decouple.

• Effectively, everything looks alike the SM, but

λ_{HHH} *can considerably differ from the SM value* $\lambda^{(0)}_{HHH}$

$\Rightarrow$

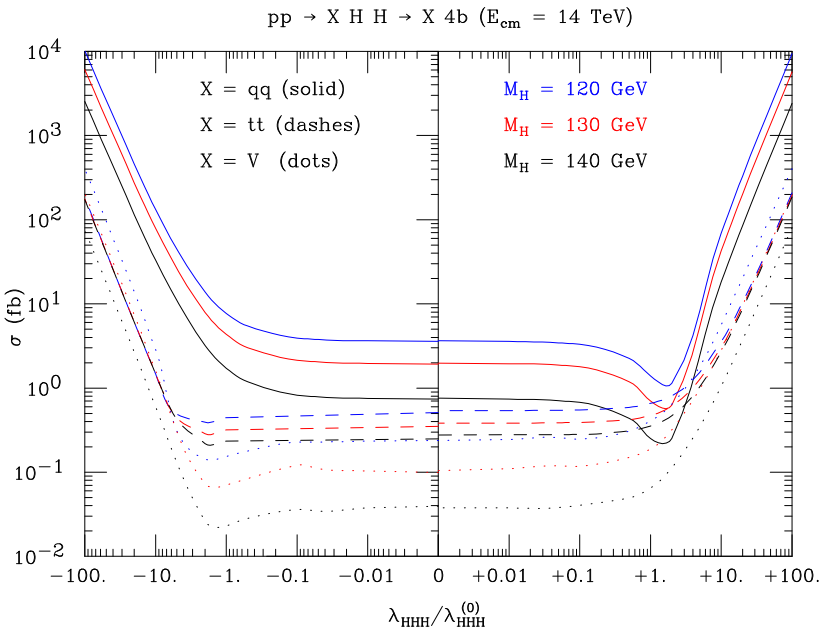

Figure 3: *Dependence of the cross sections for the three processes* $qq^{(\prime)} \to qq^{(\prime)}HH$, $gg, q\bar{q} \to t\bar{t}HH$ *and* $q\bar{q}^{(\prime)} \to VHH$ *on the triple-Higgs self-coupling, for three values of the Higgs mass.*

• This possibility can be analyzed by implementing the exact couplings of a generic 2HDM and scanning the parameter space numerically (also checking possible problems with Gauge Invariance)

• The general scan was subject to the constraints of tree-level unitarity and to the requirement that the couplings g^2_{hVV}, g^2_{htt} and g^2_{hbb} differ from the SM values by no more than 30%, 30% and 70%, respectively, and with masses of the heavy Higgs states $m_H \gtrsim 300$ GeV.

• The result of the scan is reported in the last row of the following Table, together with the computed exclusion limits

$\Rightarrow$

M_H (GeV)	120		130		140	
LHC, 95% CL	-4.8	7.5	-6.0	9.0	-9.5	12.4
SLHC, 95% CL	-1.8	3.7	-2.5	5.3	-4.4	7.4
LHC, 3σ	-6.6	9.3	-8.1	11.0	-12.4	15.4
SLHC, 3σ	-2.7	5.1	-3.6	6.5	-5.9	8.9
2HDM scan	$-8 < r < 36$		$-7 < r < 35$		$-6 < r < 34$	

Table 1: *Constraints on the ratio* $r = \lambda_{hhh}/\lambda^{(0)}_{HHH}$ *using all three channels. In the top box, the two values in each entry correspond to* $r_{\rm min}$, $r_{\rm max}$, *where* $r < r_{\rm min}$ *and* $r > r_{\rm max}$ *define the range which can be excluded at 95% CL (first row) or probed at the* 3σ *level (second row). The bottom box contains the ranges for* r *allowed by the 2HDM scan.*

- Notice that our analysis is model independent

R. Pittau

Granada, January 2007

4

NLO forward-backward charge asymmetries in $p\overset{(-)}{p} \to l^- l^+ j$ production at large hadron colliders

• Based on:

F. del Aguila, L. Ametller and R.P., Phys. Lett. B **628**, 40 (2005)

The motivation

The observables

The calculation

The results

The uncertainties

The problem of a realistic simulation

The conclusions

The motivation

- The large cross sections for gauge boson production at Tevatron and LHC might give a chance to determine the Standard Model electroweak parameters with high precision.

- In particular, charge asymmetries allow to measure the fermion couplings to the Z boson, namely $\sin^2\theta_{\rm eff}^{\rm lept}$.

- The simplest case is $A_{\rm FB}$ in the Drell-Yan process

$$q\bar{q} \to Z, \gamma^* \to l^- l^+.$$

• The associated production of a neutral gauge boson $V = \gamma, Z$ (with $V \to l^- l^+$) and a jet has also a large cross section, especially at LHC, thus can also allow for a precise determination of the effective weak mixing angle.

• This correction to V production *is a genuine new process* when the detection of the extra jet is required. In particular, gluons can be also initial states, and the large gluon content of the proton at high energy tends to make the V and Vj production cross sections of similar size.

• Then, it is worth studying the potential of the processes

$$p\overset{(-)}{p} \to l^- l^+ j$$

in providing a *new determination of* $\sin^2\theta^{\rm lept}_{\rm eff}$ including radiative $\mathcal{O}(\alpha_s)$ corrections.

• Paper:

F. del Aguila, Ll. Ametller and R. Pittau, Phys. Lett. **B628**, 40 (2005)

The observables

- $$A_{FB} = \frac{F - B}{F + B}$$

$$F = \int_0^1 \frac{d\sigma}{d\cos\theta} d\cos\theta, \quad B = \int_{-1}^0 \frac{d\sigma}{d\cos\theta} d\cos\theta\,.$$

- We consider two possible angles:

$$\cos\theta_{CS} = \frac{2(p_z^{l^-} E^{l^+} - p_z^{l^+} E^{l^-})}{\sqrt{(p^{l^-} + p^{l^+})^2}\sqrt{(p^{l^-} + p^{l^+})^2 + (p_T^{l^-} + p_T^{l^+})^2}}$$

$$\cos\theta_j = \frac{(p^{l^-} - p^{l^+}) \cdot p^j}{(p^{l^-} + p^{l^+}) \cdot p^j}\,.$$

• $\theta_{\rm CS}$ is the Collins-Soper angle (on average, the angle between l^- and the initial quark direction).

J.C. Collins and D.E. Soper, Phys. Rev. D **16**, 2219 (1977)

• θ_j is the angle between l^- and the direction opposite to the jet in the l^-l^+ rest frame.

F. del Aguila *et al.*, Phys. Rev. Lett. **89**, 161802 (2002)

• Different asymmetries can be defined:

$p\bar{p}:$	$A^{\rm CS}$	$\cos\theta = \cos\theta_{\rm CS}$
$pp:$	$A^{\rm CS}$	$\cos\theta = \cos\theta_{\rm CS} \times \frac{\lvert p_z^{e^+} + p_z^{e^-} + p_z^j \rvert}{p_z^{e^+} + p_z^{e^-} + p_z^j}$
$p\bar{p}:$	A^j	$\cos\theta = \cos\theta_j \times \frac{\lvert p_z^{e^+} + p_z^{e^-} + p_z^j \rvert}{p_z^{e^+} + p_z^{e^-} + p_z^j}$
$pp:$	A^j	$\cos\theta = \cos\theta_j$
$p\bar{p}:$	A^b	$\cos\theta = \cos\theta_j \times (-\mathrm{sign}(Q_b))$
$pp:$	A^b	$\cos\theta = \cos\theta_j \times (-\mathrm{sign}(Q_b))$

The calculation

- As an example, we consider A^b (the same for $A^{\rm CS}$ and A^j) :

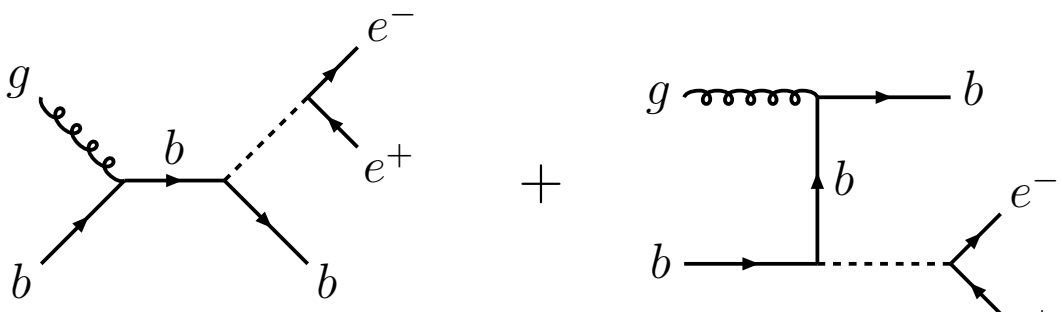

Leading Order gb and bg contributions.

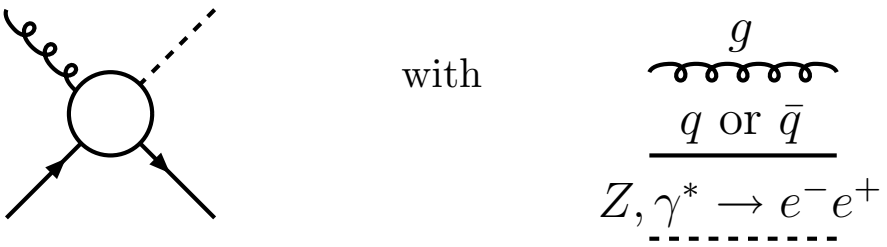

NLO Virtual gb and bg contributions.

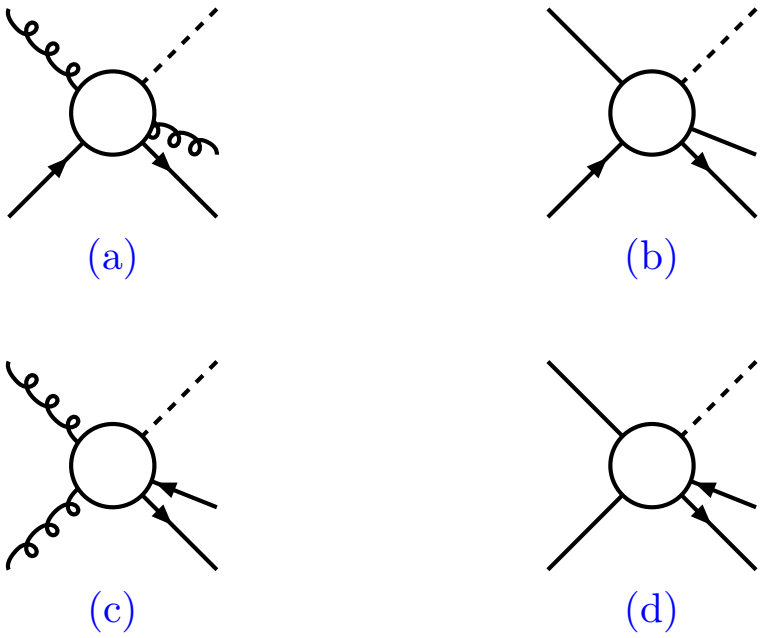

NLO Real $\underline{gb}$ *and* $\underline{bg}$ (a), $\underline{\overset{(}{\bar{q}}\overset{)}{} b}$ *and* $\underline{b\overset{(}{\bar{q}}\overset{)}{}}$ (b), $\underline{gg}$ (c), $\underline{q\bar{q}}$ *and* $\underline{\bar{q}q}$ (d) *contributions.*

- $$\mathrm{d}\sigma^{\mathrm{NLO}} = \sum_{i,j} \int_0^1 dx_1 \int_0^1 dx_2 \; f_i^{\mathrm{NLO}}(x_1) f_j^{\mathrm{NLO}}(x_2) \; \mathrm{d}\hat{\sigma}_{ij}^{\mathrm{NLO}}$$

$$i, j = g, b, q, \bar{q}$$

$$f_i^{\mathrm{NLO}}(x) = f_i^{(0)}(x) + \alpha_s f_i^{(1)}(x)$$

$$\mathrm{d}\hat{\sigma}_{ij}^{\mathrm{NLO}} = \mathrm{d}\hat{\sigma}_{ij}^{(0)} + \alpha_s \mathrm{d}\hat{\sigma}_{ij}^{(1)} \, .$$

- The size of the various terms ($L = \log \frac{\mu}{m_b}$):

a) $\left[f_g^{(0)}(x_1) f_b^{(0)}(x_2) \; \mathrm{d}\hat{\sigma}_{gb}^{(0)} + (x_1 \leftrightarrow x_2) \right] \sim \sum_{k=0}^{\infty} \alpha_s^k L^k$

b) $\alpha_s \left[f_{(g,q,\bar{q})}^{(0)}(x_1) f_b^{(0)}(x_2) \; \mathrm{d}\hat{\sigma}_{(g,q,\bar{q})b}^{(1)} + (x_1 \leftrightarrow x_2) \right] \sim \alpha_s \sum_{k=0}^{\infty} \alpha_s^k L^k$

c) $\alpha_s \left[f_g^{(0)}(x_1) f_g^{(0)}(x_2) \; \mathrm{d}\hat{\sigma}_{gg}^{(1)} + (x_1 \leftrightarrow x_2) \right] \sim \alpha_s \sum_{k=0}^{\infty} \alpha_s^k L^k$ or $\sim \underline{\alpha_s L \sum_{k=0}^{\infty} \alpha_s^k L^k}$

• The apparent double counting is resolved when considering the evolution of the parton densities:

d) $\alpha_s \left[\left(f_g^{(1)}(x_1) f_b^{(0)}(x_2) + f_g^{(0)}(x_1) f_b^{(1)}(x_2) \mathrm{d}\hat{\sigma}_{gb}^{(0)} + (x_1 \leftrightarrow x_2) \right) \right]$

$$\sim -\alpha_s L \sum_{k=0}^{\infty} \alpha_s^k L^k$$

• The separation between *Virtual* and *Real* contributions in $\mathrm{d}\hat{\sigma}_{ij}^{(1)}$ is performed with a Dipole Formalism.

S. Catani and M.H. Seymour, Nucl. Phys. **B485**, 291 (1997)

• We used `MCFM v4.1` (modified to compute A^b)

J.M. Campbell, R.K. Ellis, http://mcfm.fnal.gov/

and `ALPGEN`.

M.L. Mangano *et al.*, JHEP **0307**, 001 (2003)

The results

- Our simulation of the set up at LHC (Tevatron) for $l = e$:

$$p_t^e = \sqrt{p_T^{e\,2}} > 20\,\text{GeV}, \qquad p_t^j = \sqrt{p_T^{j\,2}} > 50\,(30)\,\text{GeV},$$
$$|\eta^{e,j}| < 2.5, \qquad \Delta R_{e,j} > 0.4\,.$$

- Parton distributions `cteq6l1` (`cteq6m`) at LO (NLO).
- A sanity check:

$$R = \frac{p\bar{p} \to V\ (\bar{b})}{p\bar{p} \to V\ j} = 0.020$$

to be compared with $R_{\text{exp}} = 0.023(5)$ measured by DØ.

V.M. Abazov *et al.*, Phys. Rev. Lett. **94**, 161801 (2005)

Contributing process	LHC		Tevatron	
	LO	NLO	LO	NLO
$g\overset{(-)}{q} \to Vj(j)$	44.3	53.4	3.40	4.77
$q\bar{q} \to Vj(j)$	8.4	} 3.7	4.61	} 2.76
$\overset{(-)}{q}\overset{(-)}{q} \to Vj(j)$	–		–	
$gg \to Vj(j)$	–		–	
Total	52.7	57.1	8.01	7.53
$gb \to Vb(g)$	1.81	} 1.81	0.038	} 0.049
$gg \to Vb(\bar{b})$	–		–	
$\overset{(-)}{q}b \to Vb(\overset{(-)}{q})$	–		–	
$q\bar{q} \to Vb(\bar{b})$	–	0.06	–	0.025
Total	1.81	1.87	0.038	0.074

Estimates for the e^-e^+j and e^-e^+b cross sections at LHC ($\sqrt{s} = 14$ TeV) and Tevatron ($\sqrt{s} = 1.96$ TeV) in pb

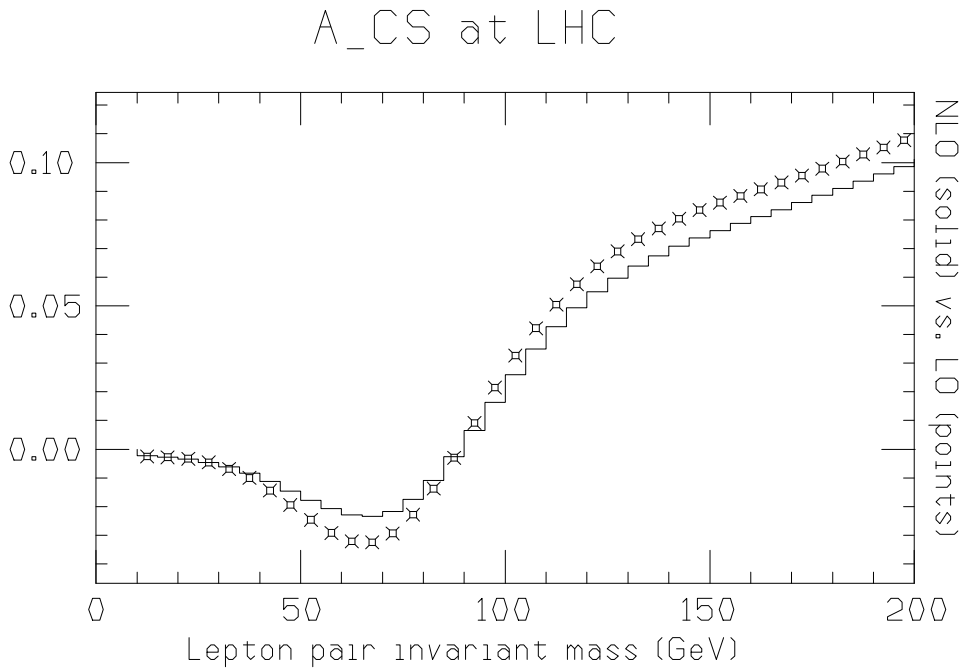
A_CS at LHC
0.10
0.05
0.00
0
50
100
150
200
Lepton pair invariant mass (GeV)
NLO (solid) vs. LO (points)

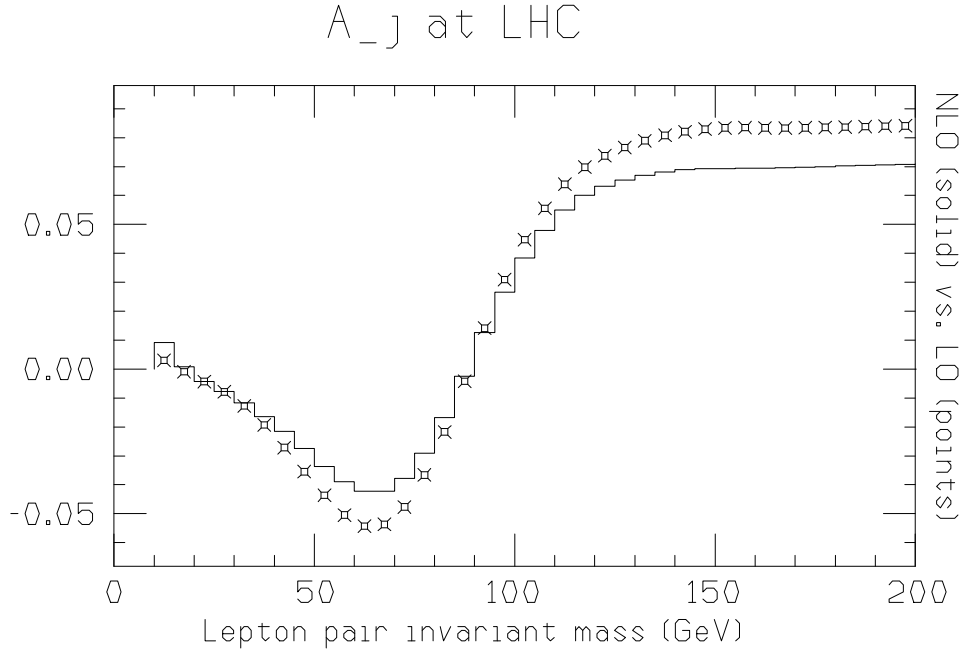
A_j at LHC
0.05
0.00
-0.05
0
50
100
150
200
Lepton pair invariant mass (GeV)
NLO (solid) vs. LO (points)

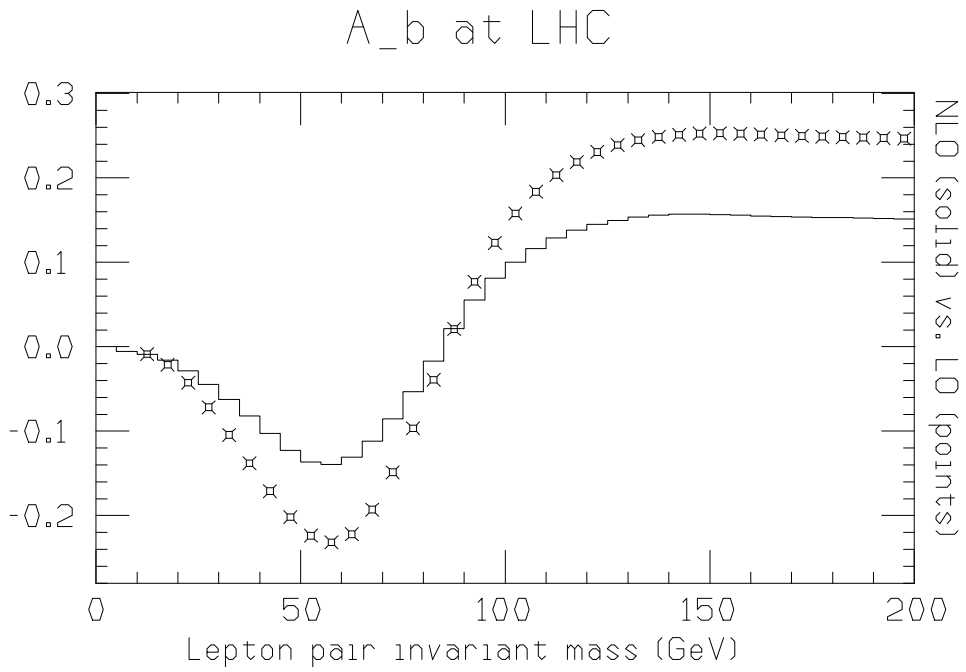
A_b at LHC
0.3
0.2
0.1
0.0
-0.1
-0.2
0
50
100
150
200
Lepton pair invariant mass (GeV)
NLO (solid) vs. LO (points)

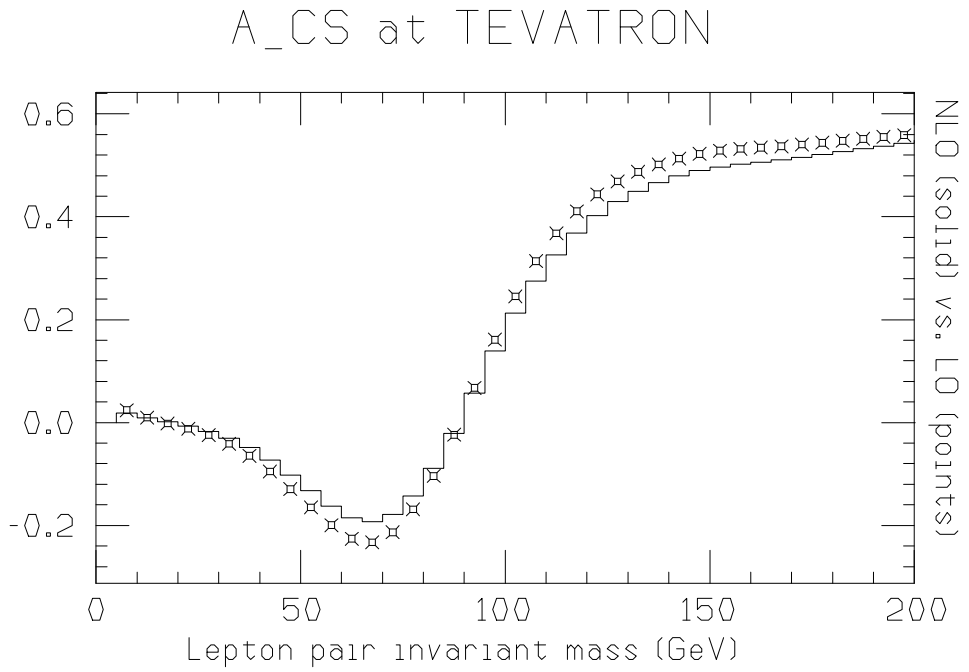
A_CS at TEVATRON
0.6
0.4
0.2
0.0
-0.2
0
50
100
150
200
Lepton pair invariant mass (GeV)
NLO (solid) vs. LO (points)

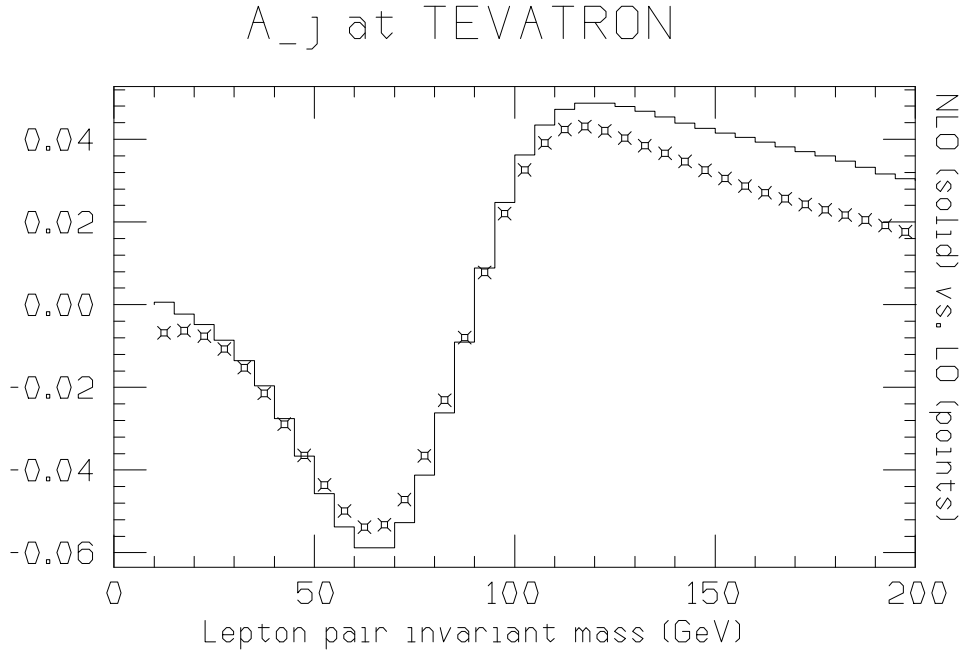
A_j at TEVATRON
0.04
0.02
0.00
-0.02
-0.04
-0.06
0
50
100
150
200
Lepton pair invariant mass (GeV)
NLO (solid) vs. LO (points)

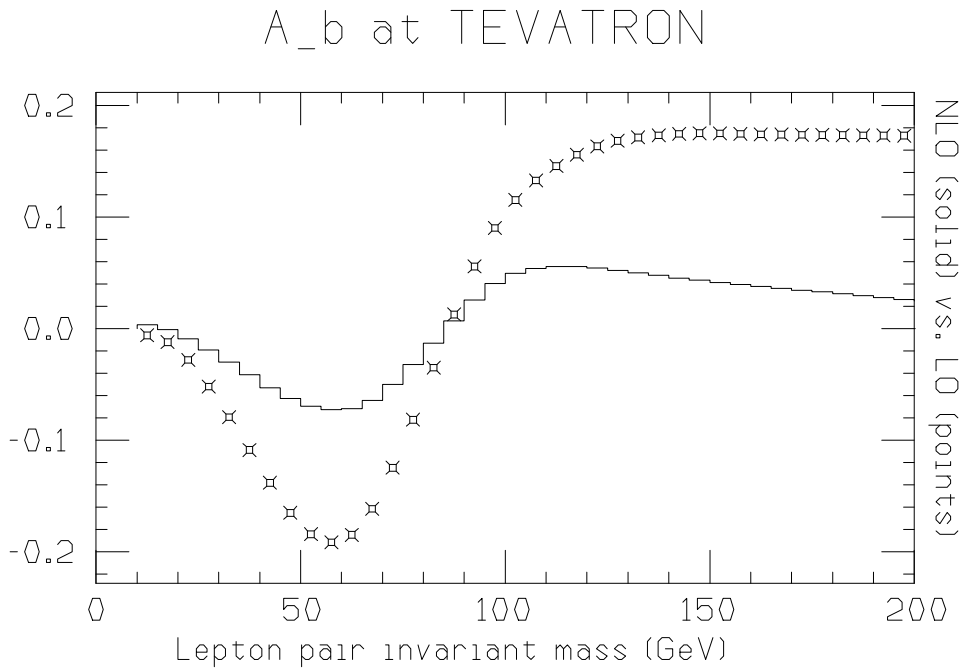
A_b at TEVATRON
0.2
0.1
0.0
-0.1
-0.2
0
50
100
150
200
Lepton pair invariant mass (GeV)
NLO (solid) vs. LO (points)

- A fit near the Z peak gives:

$$\begin{aligned} A &\sim b\,(a - \sin^2\theta_{\rm eff}) \\ \delta \sin^2\theta_{\rm eff} &\sim -\frac{\delta A}{b} \\ \delta A &\sim \sqrt{\frac{1-A^2}{N_{\rm events}}} = \sqrt{\frac{1-A^2}{L\cdot\sigma}}\,. \end{aligned}$$

- We assume an integrated Luminosity L of

$$100\ (10)\ fb^{-1}\ \text{at LHC (Tevatron)}.$$

LO/NLO	σ(pb)		A	δA	$\delta \sin^2 \theta_{\rm eff}^{\rm lept}$
LHC	$\sigma^{Vj} = 53$	$A^{\rm CS}$	8.7×10^{-3}	4.4×10^{-4}	1.3×10^{-3}
	57		6.8×10^{-3}	4.2×10^{-4}	1.3×10^{-3}
		A^j	1.2×10^{-2}	4.4×10^{-4}	8.8×10^{-4}
			1.1×10^{-2}	4.2×10^{-4}	1.1×10^{-3}
	$\sigma^{Vb} = 1.8$	A^b	7.5×10^{-2}	2.3×10^{-3}	8.7×10^{-4}
	1.9		4.9×10^{-2}	2.3×10^{-3}	1.4×10^{-3}
Tevatron	$\sigma^{Vj} = 8.0$	$A^{\rm CS}$	6.4×10^{-2}	3.5×10^{-3}	1.4×10^{-3}
	7.5		5.5×10^{-2}	3.6×10^{-3}	1.7×10^{-3}
		A^j	9.9×10^{-3}	3.5×10^{-3}	8.1×10^{-3}
			1.1×10^{-2}	3.6×10^{-3}	7.2×10^{-3}
	$\sigma^{Vb} = 0.04$	A^b	5.5×10^{-2}	5.1×10^{-2}	2.5×10^{-2}
	0.07		2.7×10^{-2}	3.7×10^{-2}	4.7×10^{-2}

The uncertainties

• In the Table we assumed a b-tagging efficiency ϵ of 100 % and *NO contamination ω in disentangling b and $\bar{b}$ jets*.

• Taking ϵ and ω into account means in practice dividing $\delta \sin^2 \theta^{\rm lept}_{\rm eff}$ coming from the Vb events by $\sqrt{\epsilon}(1-2\omega)$.

• A typical value for ϵ is 50 % while ω can be estimated as follows:

- *Once the forward and backward hemispheres are identified, event by event, with some criterion, the charge separation $\delta_b^{\rm exp}$ of the average charges measured in both hemispheres can be determined:*

$$\delta_b^{exp} = < Q_b >_F - < Q_b >_B .$$

- *On the other hand a simple calculation yields a relation among δ_b^{exp}, the bare quark charge Q_b and ω:*

$$\delta_b^{exp} = 2Q_b(1-2\omega).$$

- *Using $Q_b = -\frac{1}{3}$, together with the experimental LEP value $\delta_b^{\rm exp} = -0.21$, gives* $\omega \sim 0.34$.

• This loss of precision is partly compensated by the fact that the Table refers to b production only: adding $\bar{b}$ doubles the available statistics.

At any rate approaching the quoted precisions will be an experimental challenge.

• Another source of uncertainty is the dependence of the asymmetries on parton densities (`cteq` and `mrst`).

• Variations of the asymmetries of the order of 10% can be easily observed around the Z peak at both colliders.

• This can be considered as an extra handle provided by the asymmetry measurements in constraining the parton distribution functions.

• Conversely, with a more precise knowledge of them, the charge asymmetries can be used for precision measurements.

The problem of a realistic simulation

F. del Aguila, Ll. Ametller and R. Pittau, PoS (HEP2005) 311

• Although a complete NLO result is essential to predict the correct production rates, a realistic experimental analysis is better performed with a tree level program allowing an easier interface with parton shower and hadronization packages.

• This looks feasible in the Vj case, but the stronger impact of the NLO corrections seems to prevent that for Vb.

• A possible way out is using a program as `ALPGEN` and produce the Vb final state only through the tree level $gg \to Vb(\bar{b})$ and $q\bar{q} \to Vb(\bar{b})$ subprocesses (the former rate is finite when computed with $m_b \neq 0$).

• As a result, a good approximation to the exact asymmetries around the Z peak can be obtained:

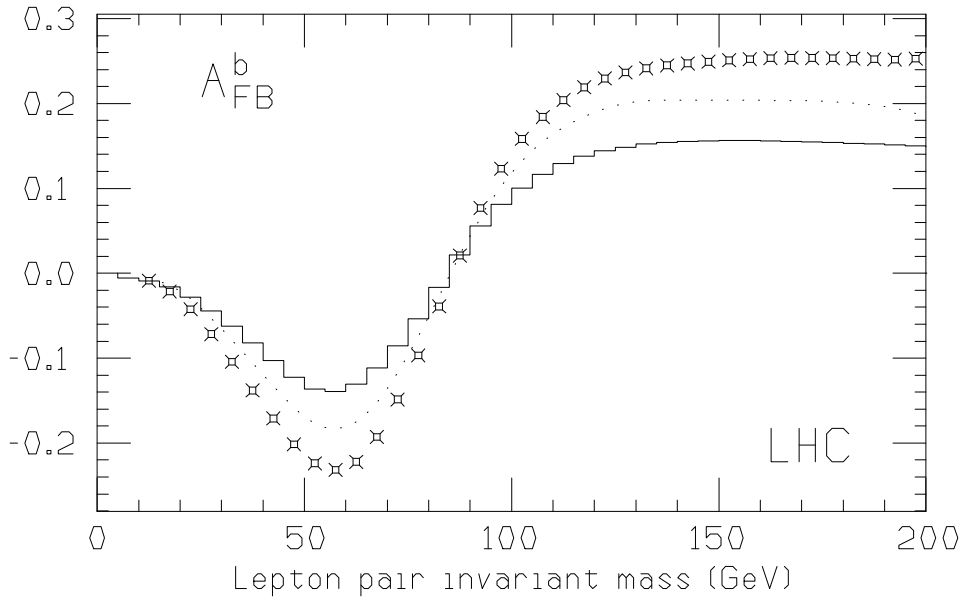

The dotted line refers to the approximation of using only ALPGEN

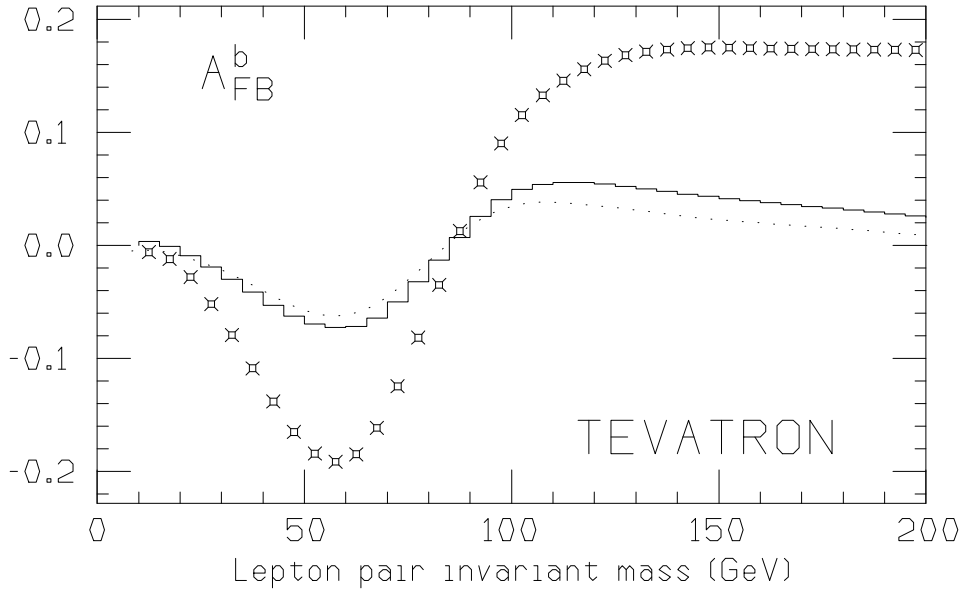

The dotted line refers to the approximation of using only ALPGEN

• As a drawback of this approach wrong rates are obtained, namely $\sigma^{Vb} = 1.0$ (0.04) pb at LHC (Tevatron) to be compared with the NLO numbers: 1.9 (0.007) pb

$\Rightarrow$ a K factor should be included

• A rather easy way to achieve this is using a fake b mass:

with $m_b \sim 1$ GeV the correct Vb production rate is reproduced at Tevatron, leaving the corresponding asymmetry nearly unchanged.

The conclusions

• Our result should be compared with the final LEP1 + SLD analysis (Winter '05):

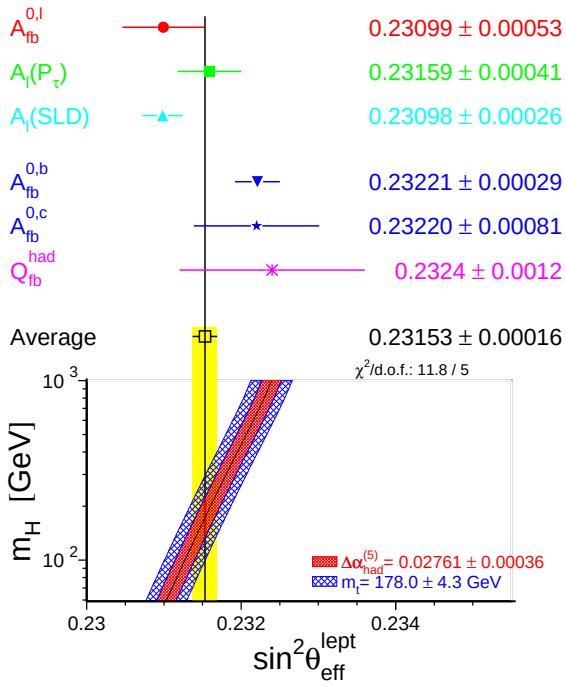

• To make contact with experiment, we quote a recent result by DØ using Drell-Yan with $72\,pb^{-1}$ of integrated luminosity:

$$\sin^2\theta_{\rm eff} = 0.2238 \pm 0.0040 \pm 0.0030\,.$$

D. Acosta *et al.*, Phys. Rev. **D71**, 052002 (2005)

• The 2 dominant backgrounds are under control:

[1] j's misidentified as $e^{\pm}$, [2] $p\bar{p} \to W^+W^- \to e^+e^-\nu_e\bar{\nu}_e$.

• In our case, *with 1 additional jet*, we need an even more demanding experimental performance. For example:

a) events with *exactly* 1 jet should be selected

b) A^b requires measuring the charge of the b quark *inside* the jet.

Even though the experimental challenge is very demanding, pursuing such measurements might provide an important and new test of the Standard Model.